DMD Fast Forward. Published on July 15, 2016 as DOI: 10.1124/dmd.116.071076
This article has not been copyedited and formatted. The final version may differ from this version.

DMD # 071076

Evaluation of CYP2B6 Induction and Prediction of Clinical DDI: Considerations from the IQ Consortium Induction Working Group- An Industry Perspective.

International Consortium for Innovation and Quality in Pharmaceutical Development (IQ). CYP2B6 Induction Working Group

Odette A Fahmi, Mohamad Shebley, Jairam Palamanda, Michael W Sinz, Diane Ramsden, Heidi J Einolf, Liangfu Chen, Hongbing Wang.

Pfizer Inc., Groton, Connecticut (OAF), AbbVie Inc., North Chicago, Illinois (MS), Merck Research Laboratories, Rahway, New Jersey (JP), Bristol Myers Squibb, Wallingford, Connecticut (MWS), Boehringer Ingelheim, Ridgefield, Connecticut (DR), Novartis, East Hanover, New Jersey (HJE); GlaxoSmithKline, King of Prussia, Pennsylvania (LC), University of Maryland School of Pharmacy, Baltimore, MD (HW).

DMD # 071076

Running title: CYP2B6 Induction and Prediction of Clinical DDI

Corresponding Author:

Odette A. Fahmi, Ph.D

Department of Pharmacokinetics, Dynamics and Metabolism, Pfizer Inc., Eastern Point Road,

Groton CT 06340; Phone: +1-860-287-0855. E-mail: odette.a.fahmi@pfizer.com

Number of text pages:	25
Number of tables:	6
Number of Supplemental tables:	5
Number of figures:	4
Number of references:	66
Number of words in Abstract:	254
Number of words in Introduction:	723
Number of words in Discussion:	1583

DMD Fast Forward. Published on July 15, 2016 as DOI: 10.1124/dmd.116.071076
This article has not been copyedited and formatted. The final version may differ from this version.

Abbreviations:

Pregnane-X Receptor (PXR)

Constitutive Androstane Receptor (CAR)

Drug-Drug Interactions (DDI)

Cytochrome P450 (CYP)

Area under the concentration curve (AUC)

European Medicines Agency (EMA)

Food and Drug Administration (FDA)

International Consortium for Innovation and Quality in Pharmaceutical Development (IQ)

New Molecular Entity (NME)

Maximum fold increase over vehicle control (E_{max})

In vitro concentration of inducer that produced half the maximum induction (EC_{50})

Enzyme Inhibition Constant (K_i)

Time Dependent Inhibition (TDI)

Inhibitor Concentration at 50% of kinact (K_I)

Maximal Inactivation Rate (k_{inact})

In vitro-in vivo extrapolation (IVIVE)

Relative Induction Score (RIS)

Physiologically-Based Pharmacokinetics (PBPK)

Geometric Mean Fold Error (GMFE)

Uridine 5'-diphospho-glucuronosyltransferases (UGTs)

Trans-2-phenylcyclopropylamine Hydrochloride (PCPAH)

ABSTRACT

Drug-drug interactions (DDI) due to CYP2B6 induction have recently gained prominence and clinical induction risk assessment is recommended by regulatory agencies. The objective of this work was to evaluate the potency of CYP2B6 vs CYP3A4 induction *in vitro* and from clinical studies, and to assess the predictability of efavirenz vs bupropion as clinical probe substrates of CYP2B6 induction. The analysis indicates that the magnitude of CYP3A4 induction was higher than CYP2B6 both *in vitro* and *in vivo*. The magnitude of DDI caused by induction could not be predicted for bupropion with static or dynamic models. On the other hand, the RIS, Net Effect, and SimCYP models using efavirenz resulted in improved DDI predictions. Although bupropion and efavirenz have been used and are recommended by regulatory agencies as clinical CYP2B6 probe substrates for DDI studies, CYP3A4 contributes to the metabolism of both probes and is induced by all reference CYP2B6 inducers. Therefore, caution must be taken when interpreting clinical induction results due to lack of selectivity of these probes. While IVIVE for efavirenz performed better than bupropion, interpretation of the clinical change in exposure is confounded by the co-induction of CYP2B6 and CYP3A4, and the increased contribution of CYP3A4 to efavirenz metabolism under induced conditions. Current methods and probe substrates preclude accurate prediction of CYP2B6 induction. Identification of a sensitive and selective clinical substrate for CYP2B6 (f_m > 0.9) is needed to improve IVIVE for characterizing the potential for CYP2B6 mediated DDI. Alternative strategies and a framework for evaluating the CYP2B6 induction risk are proposed.

INTRODUCTION

Given the importance of drug-drug interactions (DDI) in the overall clinical safety profile of medications, the U.S. Food and Drug Administration (FDA) (FDA (2012), the Ministry of Health, Labor and Welfare (MHLW), and the European Medicines Agency (EMA) (EUROPEAN MEDICINES AGENCY (EMA, 2012), each provided guidance documents to industry for evaluating drug interactions, which also included recommend procedures for predicting DDIs. Analogous to the regulatory guidance, several groups have published articles from an industrial perspective on how best to predict DDIs caused by inhibition and induction of drug-metabolizing enzymes with a focus on cytochrome P450 (CYP) 3A4 (Fahmi et al., 2010b; Einolf et al., 2014; Vieira et al., 2014). Throughout the regulatory guidance, DDI related to CYP interactions are analyzed and interpreted in a similar fashion with no distinction between CYP isoforms. However, in the area of enzyme induction and prediction of DDI there is a need for understanding if the predictability of current data analysis methods and interpretation using these methods are similar across CYP enzymes. Therefore, following on previous literature with CYP3A4 mediated enzyme induction (Fahmi et al., 2008b; Fahmi et al., 2009; Einolf et al., 2014), an assessment of data analysis methods to predict DDI caused by enzyme induction of CYP2B6 would be of value. In order to identify the utility of CYP2B6 *in vitro* induction data, the International Consortium for Innovation and Quality in Pharmaceutical Development (IQ Consortium) launched a CYP2B6 Induction Working Group. The IQ consortium is an organization of pharmaceutical and biotechnology companies providing a forum to address issues for the biopharmaceutical industry. This White Paper presents observations from the working group and provides an initial framework on issues and approaches to consider when evaluating the induction of CYP2B6.

CYP2B6 is one of the highly-inducible and polymorphic CYP isoforms expressed predominantly in human liver (Zanger et al., 2007; Wang et al., 2008). To date, large variations in CYP2B6 due to induction and polymorphisms have been demonstrated in humans. Inter-individual differences in hepatic CYP2B6 expression level and activity have been reported to vary up to several hundred fold (Ekins et al., 1998; Faucette et al., 2000). As such, inter-individual differences in CYP2B6 catalytic capacity may result in variable systemic exposure to drugs that are metabolized by CYP2B6, including the antineoplastic drugs, cyclophosphamide and ifosfamide (Roy et al., 1999); the antiretrovirals nevirapine and efavirenz (Ward et al., 2003); the anesthetics, propofol and ketamine (Court et al., 2001); and the anti-Parkinsonian, selegiline (Hidestrand et al., 2001). Although CYP2B6 does not play a major role in the metabolism (elimination) of many marketed drugs, efavirenz and bupropion are two drugs described in the literature and in regulatory guidance documents as sensitive probe substrates to date for the assessment of CYP2B6 enzyme activity *in vitro* and *in vivo*.

During the past ten years, important advances have been made in our understanding of the mechanisms that regulate induction of hepatic CYP2B6. The constitutive androstane receptor (CAR, NR1I3) has been identified as the primary mediator for drug-induced expression of CYP2B6, while the pregnane X receptor (PXR, RN1I2) is predominantly responsible for CYP3A4 induction (Lehmann et al., 1998; Sueyoshi et al., 1999). Nevertheless, these two closely related nuclear receptors can recognize and bind to response elements located in both CYP2B6 and CYP3A4 promoters (Xie et al., 2000; Faucette et al., 2007). The cross-talk between CAR and PXR (Zanger et al., 2007) results in shared mechanisms of transcriptional regulation of CYP2B6 and CYP3A4 and many known CYP2B6 inducers also increase the expression of CYP3A4 (Fahmi et al., 2010a; Tolson et al., 2010).

It is evident that drug-induced expression of CYP2B6 contributes to the highly variable CYP2B6 expression in human liver. However, the majority of data evaluating CYP2B6 induction have been obtained from sparse *in vitro* cell-based experimental systems and clinical DDI results. Reliable and predictive *in vitro-in vivo* extrapolation (IVIVE) models, combining more comprehensive clinical data sets with extensive *in vitro* experimental results, would be highly desirable. To that end, this manuscript describes assessments of the potency of CYP2B6 vs CYP3A4 induction *in vitro* and from clinical studies, the reliability of efavirenz vs bupropion as clinical probe substrates for CYP2B6 induction and the performance of various data analysis methods (FDA Basic R3 model, Relative Induction Score (RIS), Net Effect model, and the physiologically-based pharmacokinetics (SimCYP) model to predict the clinical outcome of CYP2B6 enzyme induction mediated DDI.

MATERIALS and METHODS

Reagents

Bupropion, cimetidine, carbamazepine, efavirenz, indinavir, nelfinavir, itraconazole, nifedipine, nevirapine, phenobarbital, phenytoin, rifampin, ritonavir, erythromycin, ticlopidine, Trans-2-phenylcyclopropylamine Hydrochloride (PCPAH), telmisartan, β-glucuronidase, glucose 6-phosphate, NADPH, and saquinavir were purchased from Sigma-Aldrich (St. Louis, MO). ^{14}C-efavirenz was purchased from Moravak Biochemical (Brea, CA). Efavirenz metabolites were purchased from Toronto Research Chemicals (Toronto, Canada). HepatoPac plates were purchased from Ascendance Biotechnology, Inc., formerly Hepregen (Medford, MA). RNeasy Mini Kit was from QIAGEN (Valencia, California) and cDNA Reverse Transcription Kit was obtained from ABI (Applied Biosystems, Foster City, CA). Pooled human liver microsomes (150 donor pool) were purchased from Gentest/Corning Discovery Labware, Woburn, MA. All

DMD Fast Forward. Published on July 15, 2016 as DOI: 10.1124/dmd.116.071076
This article has not been copyedited and formatted. The final version may differ from this version.

cell culture reagents were purchased from Life Technologies (Carlsbad, CA) unless otherwise noted.

Culture of cryopreserved human hepatocytes

Various lots of human cryopreserved hepatocytes (Supplemental Table 4) were obtained from different commercial vendors including CellzDirect (Durham, NC), Bioreclamations *In vitro* Technologies (Baltimore, MD) and XenoTech LLC, (Kansas City, KS). As detailed in previous publications (Fahmi et al., 2010a, Ramsden et al., 2015), cryopreserved human hepatocytes (Supplemental Tables 1 and 4) were thawed in hepatocyte thawing medium and were seeded in collagen I coated 24- or 96-well plates at cell densities of 0.5-1×10^6 viable cells per well in hepatocyte plating medium. Viability, as determined by trypan blue exclusion or other methods, was 85% or better when cells were plated. The cells were initially maintained at 37°C in a humidified incubator with 95% atmospheric air and 5% CO_2 overnight in hepatocyte incubation media. Following overnight incubation, the cells were treated with various compounds. Compounds were dissolved in DMSO and added to the culture medium at various concentrations (final DMSO concentration, 0.1%). After daily treatment for 2 days, the medium was removed, and the cells were washed with saline. The cells were lysed in lysis buffer and prepared for RNA isolation. Cell viability was assessed by visual inspection of the monolayer, checking for confluency and morphology. Different companies used different plating conditions and a representation of the conditions is shown in Supplemental Table 1.

RT-PCR and quantification of CYP3A4 and CYP2B6 mRNA

Following the isolation of RNA using commercially available kits, cDNA was synthesized using standard PCR protocols. CYP3A4, CYP2B6, and an endogenous probe such as glyceraldehyde 3-phosphate dehydrogenase [GAPDH] mRNA levels were quantified by real

DMD Fast Forward. Published on July 15, 2016 as DOI: 10.1124/dmd.116.071076
This article has not been copyedited and formatted. The final version may differ from this version.

time PCR. The gene-specific primer/probe sets were obtained from Applied Biosystems Incorporated (Foster City /CA) and real time PCR performed using CYP3A4, CYP2B6, and the endogenous control target cDNA's. The relative quantity of the target cDNA compared with that of the control GAPDH was determined by the ΔΔCt method (Applied Biosystems User Bulletin #2). Ct values >32 were excluded from the analysis. Relative quantification measures the change in mRNA expression in a test sample relative to that in a vehicle control sample (0.1% DMSO).

Determination of E_{max} and EC_{50} values

The *in vitro* induction mRNA data were fitted using the sigmoid 3-parameter equation (shown below) using commercially available software (e.g. Sigma Plot (San Jose/CA), or GraphPad Prism (La Jolla/CA) for the calculation of E_{max} (maximum fold-increase over vehicle control) and EC_{50} (the *in vitro* concentration of inducer that produced half the maximum induction) values.

$$\text{Induction Response} = Emax/(1+Exp(-([I]-EC50)/slope))$$

Kinetic parameters (EC_{50} and/or E_{max}) estimated from a particular donor that showed high standard error (>100% of the estimated value) were excluded from the analysis. Mean values of the pooled data gathered from different companies were used in the analysis (Table 3 and Supplemental data Tables 2 and 3).

*E*favirenz metabolism using induced long term HepatoPac model

Long term hepatocytes "hepatoPac" were purchased from Ascendance Biotechnology, Inc., formerly Hepregen. HepatoPac® products ("hepatocytes") are micropatterned to create proprietary patterns of hepatocyte "islands" surrounded by supportive stromal cells. This

DMD Fast Forward. Published on July 15, 2016 as DOI: 10.1124/dmd.116.071076
This article has not been copyedited and formatted. The final version may differ from this version.

technology replicates the physiological microenvironment of the liver and allows the hepatocytes to exhibit normal metabolic activity for over four weeks.

Human hepatocytes were induced with **[**^{14}C]-efavirenz (final concentration of 10 µM) in a 24 or 96 well plate format for 96-120 hrs, using 4 hepatocyte donors (Table 4 and Supplemental Table 4). Induced human HepatoPac plates were then further incubated with and without inducers for 72 hr (10 µM rifampin, 10 µM efavirenz, or 100 µM carbamazepine) or inhibitors (50 µM erythromycin, 10 µM ticlopidine, 10 µM telmisartan, or 10 µM PCPAH) with a total volume of 400 uL per well. At 24, 96 hr and 120 hr, 800 uL of reaction termination solution (99.9% acetonitrile and 0.1% acetic acid) was added to the wells and the cells were scraped from the bottom of the well. These samples were then transferred to 2 mL Fisher low non-specific binding vials (Fisher scientific, Pittsburg PA). Removal of cell monolayers was confirmed microscopically. After centrifugation, the supernatants were analyzed by LC-radio chromatography-MS/MS for quantitative metabolite identification. Samples of [^{14}C] efavirenz were analyzed by UPLC-LTQ Orbitrap (Thermo Scientific, San Jose, CA) coupled with a flow scintillation radiomatic detector (Perkin Elmer). Metabolite separation was achieved using a Phenomenex Gemini C_{18}, 3 µm, 150 x 4.6 mm column (Torrance, CA) with gradient elution. The mobile phase consisted of 95:5 (v/v) water/acetonitrile and 95:5 (v/v) acetonitrile/water. Both mobile phases contained 0.1% acetic acid. The samples generated from incubation of ^{14}C-efavirenz with HepatoPac were analyzed by LTQ Orbitrap for metabolite identification using high resolution full-scan MS aligned with radiometric chromatograms. The MS/MS scans (at high or unit resolution) were conducted to identify structures of metabolites. The peak areas of metabolites and parent generated from the radiometric chromatograms and their relative exposures were calculated as the percentage of the total drug related exposure. Where

DMD Fast Forward. Published on July 15, 2016 as DOI: 10.1124/dmd.116.071076
This article has not been copyedited and formatted. The final version may differ from this version.

possible, confirmation of metabolite structures was performed using authentic standards and for the glucuronide conjugates by deconjugation with glucuronidase.

Determination of k_{obs}, k_{inact}, and K_I values for CYP2B6 and CYP3A4

An IC_{50} shift assay for CYP2B6 was first conducted as a screen for identifying potential for time-dependent inhibition (TDI) (data not shown) as previously reported (Bjornsson et al., 2003). For select compounds (IC_{50} shift of >1.5), definitive kinetic parameters K_I and k_{inact} were obtained. *In vitro* kinetic parameters for time-dependent inactivation of CYP2B6 or CYP3A4 in human liver microsomes were determined for each compound by pre-incubating pooled human liver microsomes (typically 0.5 or 1 mg protein/mL) with various concentrations of the test compounds in 100 mM potassium phosphate buffer (pH 7.4) containing $MgCl_2$ (5 mM) and NADPH for an incubation period ranging from 0 to 30 min. Aliquots of the preincubation mixture were removed at various time points and diluted 20-fold with the same buffer containing bupropion or midazolam at V_{max} concentrations and NADPH. The incubation was continued for an additional 6 min to monitor the extent of bupropion or midazolam hydroxylation using LC-MS/MS. The first order rate constants (k_{obs}) for inactivation at various concentrations were calculated from the negative slope of the lines by linear regression analysis of the natural logarithm of the remaining activity as a function of time. The k_{inact} and K_I (concentration of the inhibitor that produces half maximal rate of inactivation) values were calculated (Table 3) by nonlinear regression analysis: $k_{obs} = k_{inact} \times [I]/(K_I + [I])$ (Einolf et al., 2014).

Data collection of the clinical drug interaction studies

CYP2B6 *in vivo* DDI data used in this analysis were gathered from the University of Washington database. The compiled clinical data contained 14 and 16 clinical studies, using bupropion and efavirenz as the substrate, respectively (Tables 1 and 2).

DMD Fast Forward. Published on July 15, 2016 as DOI: 10.1124/dmd.116.071076
This article has not been copyedited and formatted. The final version may differ from this version.

Net Effect model

The previously reported equation for the combined mathematical model was used in this analysis with some modifications (Fahmi et al., 2008b). Since CYP2B6 is not known to be expressed in the intestine, the liver term only was used, as shown below. Also, the TDI term was eliminated from the equation since there was no CYP2B6 TDI observed *in vitro* with the selected test compounds in this study. The net effect equation is expressed as the ratio of area under the concentration – time curve in the presence (AUC'_{po}) and absence (AUC_{po}) of a pharmacokinetic drug-drug interaction.

$$\frac{AUC'_{po}}{AUC_{po}} = \left(\frac{1}{[B \times C] \times f_m + (1 - f_m)} \right)$$

"B" is the term for induction in the liver

$$B = 1 + \frac{d \bullet E_{max} \bullet [I]_H}{[I]_H + EC_{50,I}}$$

"C" is the term for reversible inhibition in the liver

$$C = \frac{1}{1 + \frac{[I]_H}{K_i}}$$

$[I]_H$ represents concentrations of inducer relevant for liver utilizing the unbound systemic $C_{max,}$ scaling factor "d" were 0.50 and 1 with efavirenz and bupropion, respectively. The f_m CYP2B6 values used in the Net Effect static model were 0.64 and 0.50 consistent with Simcyp default values for efavirenz and bupropion, respectively. The bias of the different prediction approaches was assessed by calculation of the Geometric mean folds error (GMFE) of the data, as previously described (Fahmi et al., 2009).

DMD Fast Forward. Published on July 15, 2016 as DOI: 10.1124/dmd.116.071076
This article has not been copyedited and formatted. The final version may differ from this version.

Physiologically-based pharmacokinetics (PBPK) modeling

The mean E_{max} and EC_{50} values for CYP2B6 and CYP3A4, calculated from all the mRNA induction assessments for each perpetrator, as well as the inhibition parameter K_i, K_I and k_{inact} values were used in the PBPK modeling. Simulations for bupropion and efavirenz as victim drugs (shown in Tables 5 & 6) were assessed using SimCYP^{TM} version 14.1 and version 15.1, respectively without normalization of the *in vitro* data. However, we fully characterized the CYP2B6 *in vitro* induction potential of the inducers (Supplemental Table 2) and unlike the extensive wealth of clinical data described for CYP3A4 induction by rifampin, CYP2B6 clinically validated data are lacking to attempt normalization. The victim bupropion compound default file was available in SimCYP^{TM} version 14.1, and the efavirenz compound default file utilized SimCYP version 15.1. Efavirenz SimCYP file was updated with the newly generated *in vitro* parameters (K_i, K_I, k_{inact}, EC_{50} and E_{max}) for both CYP3A4 and CYP2B6 (Table 3). Perpetrators with available model files within the SimCYP compound library were updated with newly generated CYP2B6 and CYP3A4 induction data (without normalization to rifampin (Ke et al., 2016) and/or any missing inhibition/inactivation kinetic parameters, as shown in Table 3. Perpetrator compounds that had to be built were validated using published clinical pharmacokinetic information to ensure the models reasonably recapitulated day 1 plasma concentration-time profiles reported in the clinical trials (Supplemental Table 5).

RESULTS

Data analysis of the clinical drug-drug interaction studies

CYP2B6 *in vivo* DDI data used for this analysis are presented in Tables 1 and 2. The compiled clinical data contained 14 clinical studies using bupropion as the substrate with 7 precipitants,

16 studies using efavirenz as the substrate with 9 precipitants and 4 precipitants were administered with both substrates. In all cases, precipitant and victim drugs were administered orally. In 17 out of 30 clinical trials there was no clinically relevant interaction observed according to the bioequivalence criteria in the FDA DDI guidance (FDA, 2012) (AUCR = 0.8-1.25). The most pronounced change in AUCR was mediated by carbamazepine with bupropion as a probe substrate (AUCR = 0.1). Moderate induction was mediated by 4 of 12 precipitants, namely efavirenz, rifampin, ritonavir, and nevirapine. The magnitude of change observed with rifampin was largely dependent on the efavirenz dosing regimen (single dose or multiple doses). For ritonavir, a dosage of 600 mg daily for > 1 week caused the most pronounced decrease in bupropion AUC (up to AUCR 0.34), and negligible change in efavirenz exposure when 100 mg was administered for 7 days. Similarly rifampin caused a greater reduction in bupropion AUC than efavirenz, especially when efavirenz was administered as a single dose (AUCR = 0.44-0.61) vs multiple doses (AUCR = 0.63-0.82).

In vitro kinetic parameter determination

In vitro induction parameters based on mRNA were generated across multiple companies and data were pooled for each inducer (Table 3 and Supplemental Tables 1- 4). For compounds where inhibition was observed, *in vitro* IC_{50} and K_I/k_{inact} values were also generated. The induction parameters for each inducer were determined from at least two companies and multiple hepatocytes donors (supplemental Tables 1-4), and the results are presented as averages. Also, commonly used *in vitro* CYP2B6 prototypical inducers such as phenobarbital and phenytoin were included for comparisons with the *in vitro* profiles determined for the clinical inducer data set.

Inducers that are selectively targeting CYP2B6 were not identified. In contrast, co-induction of CYP3A4 was observed for all tested CYP2B6 inducers. Of note, the EC_{50} values for CYP2B6

DMD Fast Forward. Published on July 15, 2016 as DOI: 10.1124/dmd.116.071076
This article has not been copyedited and formatted. The final version may differ from this version.

induction were lower than CYP3A4 with all compounds except for rifampin. CYP2B6 and CYP3A4 induction parameters for itraconazole and cimetidine could not be determined due to lack of detectable induction *in vitro*. CYP3A4 was more sensitive to induction by rifampin (lower EC_{50}, higher E_{max}) than CYP2B6. The EC_{50} and E_{max} ratios for CYP3A4/CYP2B6, E_{max} and EC_{50}, were calculated in order to evaluate the relative potency of CYP2B6 vs CYP3A4 induction. In all cases the ratio of CYP3A4/CYP2B6 E_{max} was > 1 (range 1.4-3.9), confirming that the magnitude of induction mediated for CYP3A4 at the mRNA level is higher than CYP2B6 *in vitro* (Table 3), and consistent with previously published data (Faucette et al., 2007; Fahmi et al., 2010a). Although, it is worth noting that previously reported data with nevirapine and efavirenz showed higher induction of CYP2B6 than CYP3A4, which may be due to the shorter (24-hr) hepatocytes treatment time with test compounds (Faucette et al. 2007). Applying the same comparison to EC_{50} values demonstrated that EC_{50} values between CYP2B6 and CYP3A4 were similar for carbamazepine, indinavir, nelfinavir, and phenobarbital. EC_{50} values were higher for CYP3A4 than CYP2B6 for efavirenz, nevirapine, saquinavir, terifluomide, and phenytoin. Only rifampin had a lower EC_{50} for CYP3A4 than for CYP2B6. Interestingly, the change in enzyme activity for CYP2B6 tended to be similar to the fold increase in mRNA whereas CYP3A4 mRNA increases were typically higher than corresponding activity (data not shown).

f_m values for the clinical substrates bupropion and efavirenz

Initial estimations using the *in vitro* derived induction parameters and published IVIVE models for characterizing clinical induction resulted in poor predictions, particularly for bupropion. Based on the currently available literature the lack of IVIVE capability for bupropion was likely due to the lack of selectivity of this probe towards CYP2B6. The same data was not available for efavirenz and additionally there are no strong *in vivo* inhibition studies to validate the f_m for

DMD Fast Forward. Published on July 15, 2016 as DOI: 10.1124/dmd.116.071076
This article has not been copyedited and formatted. The final version may differ from this version.

CYP2B6 towards overall efavirenz metabolism. Therefore an attempt was made to understand the contribution of CYP2B6 in metabolizing efavirenz at its clinically relevant induced steady state concentration (10 μM) in order to evaluate the impact of co-induction of CYP2B6 and CYP3A4 on the metabolism through these pathways. The study was designed based on available metabolite identification data and published pathways for clearance of efavirenz.

Efavirenz metabolism using the HepatoPac *in vitro* model

A long-term incubation of a human hepatocyte model (HepatoPac) (Ramsden et al., 2015; Sane et al., 2015) was used to identify the contribution of CYP2A6, CYP2B6, CYP3A4 and UGT (predominately UGT2B7) towards efavirenz metabolism (di Iulio et al., 2009; Kwara et al., 2009; Ogburn et al., 2010; Court et al., 2014) (Table 4). Induced human HepatoPac (with 10 μM ^{14}C-efavirenz) plates were then further incubated with and without inducers for 72 hr (10 μM rifampin, 10 μM efavirenz, or 100 μM carbamazepine) or inhibitors (50 μM erythromycin, 10 μM ticlopidine, 10 μM telmisartan, or 10 μM PCPAH). Where possible, confirmation of metabolite structures was performed using authentic standards and for the glucuronide conjugates by deconjugation with glucuronidase. The metabolic profile was in line with literature reports and metabolites identified were 8-hydroxy, 8,14-di-hydroxy, 8-hydroxyglucuronide, 8,14- di-hydroxyglucuronide, 7-hydroxy, 7-hydroxyglucuronide and efavirenz N-glucuronide, while 7-hydroxysulphate was not detected.

When human hepatocytes were incubated to the induced state (96-120 hr incubation with ^{14}C-efavirenz), the average extent of efavirenz depletion by metabolism across donors was 47% (n=4), with the primary metabolic route being through the 8-OH pathway (primarily recovered as the glucuronide conjugate), followed by the 7-OH pathway (primarily recovered as the glucuronide conjugate) and lastly through N-glucuronidation, as shown in Table 4).

DMD Fast Forward. Published on July 15, 2016 as DOI: 10.1124/dmd.116.071076
This article has not been copyedited and formatted. The final version may differ from this version.

When hepatocytes were treated with [^{14}C]-efavirenz (for up to 120 hr) and allowed to be induced further for 72 hr with either rifampin (10 µM) or carbamazepine (100 µM), only carbamazepine resulted in a pronounced increase in efavirenz depletion by metabolism (≈2-fold greater depletion than solvent control) and increased in the 8-OH pathway only, in line with it being an inducer of CYP2B6 and CYP3A4. There was no increase in efavirenz metabolism with the extended rifampin or efavirenz treatment, suggesting that efavirenz auto-induction resulted in the maximal change in CYP2B6/CYP3A4 expression, which is consistent with the clinical observations (Table 2). The difference between carbamazepine and rifampin highlights the overlapping regulation of CYP2B6 and CYP3A4, and their contributions to efavirenz metabolism upon induction. The clinical DDI data showed a difference in magnitude of efavirenz AUCR (with/without rifampin) when multiple efavirenz doses were given (0.63- to 0.82) versus when a single dose was given (0.44-to 0.61), as shown in Table 2.

In the *in vitro* study, the extent of efavirenz metabolism was decreased suggesting a potential inhibitory effect by rifampin or other factors for example increased exposure of efavirenz by rifampin has been observed in clinical studies and was associated in part with CYP2B6 polymorphisms (Kwara et al., 2014). Inhibition of CYP2A6 metabolism confirmed that formation of 7-OH metabolite was mediated predominately by CYP2A6 (94% inhibition of 7-OH pathway relative to the solvent control). Inhibition of CYP2A6 increased the 8-OH pathway and decreased the N-glucuronidation.

Inhibition of CYP2B6 metabolism decreased the 8-OH pathway by 76% relative to the solvent control, while increasing the metabolism through the 7-OH pathway from 88% relative to the solvent control, suggesting that this may serve as a compensatory pathway for efavirenz metabolism.

DMD Fast Forward. Published on July 15, 2016 as DOI: 10.1124/dmd.116.071076
This article has not been copyedited and formatted. The final version may differ from this version.

Selective inhibition of CYP3A4 by erythromycin resulted in a decrease the 8-OH pathway by 54% relative to cells treated with solvent control. Both the 7-OH pathway and N-glucuronidation pathways were increased to 22% and 54% relative to cells treated with solvent control, respectively. These data confirm that CYP3A4 plays an important role also in the formation of 8-OH efavirenz. When a *pan*-UGT inhibitor, telmisartan, was added, glucuronidation was significantly inhibited. Formation of efavirenz N-glucuronide decreased by 98% relative to cells treated with solvent control. There was minimal effect on the 8-OH pathway. However, the 7-OH pathway increased to 48% relative to cells treated with solvent control, as described in Table 4.

R3 model

The R3 equation $R3=1/(1+E_{max}[I]/(EC_{50}+[I]))$ described in the FDA guidance was used for comparison with observed clinical DDI. The R3 equation uses total (bound + unbound) C_{max} as the inducer input parameter, [I]. The R3 approach typically represents a conservative estimate of AUCR. Resulting R3 values are displayed in Tables 5 and 6 for bupropion and efavirenz, respectively. Comparing the R3 predictions with the observed AUCR for bupropion and efavirenz resulted in an over-prediction of DDI (Figure 1). Despite that there were no false negatives; the percent of false positives were 44% and 29% for efavirenz and bupropion, respectively.

RIS model

A correlational approach was used to predict clinical DDI using RIS calibration curves (RIS for each precipitant drug = $E_{max}[I]/(EC_{50}+[I]$. The RIS equation uses unbound C_{max} as the inducer input parameter [I]. This approach uses various inducers with a wide range of induction potencies in order to generate a correlation curve between *in vitro* RIS values and observed

AUCR changes (Fahmi et al., 2008a). RIS calibration curves were attempted for bupropion (Poster presented at the ISSX meeting by Sun et al., 2014) and efavirenz using observed clinical AUCR values. The RIS model with bupropion could not be established, while with efavirenz a reasonable correlation (R^2 = 0.866) was established (Figure 2 and Tables 5 and 6).

Net effect modeling and comparison to clinical outcome

The mechanistic static net effect model described in the EMA and FDA guidance's (EMA, 2012; FDA, 2012), (Fahmi et al., 2008b) and as described in the methods section was used to predict AUCR for CYP2B6-mediated induction (Figure 3). This model incorporates concomitant DDIs such as competitive and time dependent inhibition along with induction kinetic parameters, in addition to a calculated scalar for *in vitro* induction data (d-factor). The f_m CYP2B6 values used in the Net Effect static model were 0.50 and 0.64, for bupropion and efavirenz, respectively. The magnitude of DDI could not be accurately predicted with bupropion. Efavirenz resulted in better predicted values (d=0.50), without any observed false negatives or false positives. However, clinical studies using multiple doses of efavirenz were excluded (n=3), due to the limitation of the Net effect model of using one concentration rather than time-based concentration profile, and the inability to account for auto-induction of the probe substrate (Figure 3 and Tables 5 & 6).

PBPK modeling and comparison to clinical outcome utilizing SimCYP

A mechanistic dynamic modeling approach was performed using SimCYP. Results are displayed in Tables 5 and 6, and graphically in Figure 4. The magnitude of DDI for bupropion tended to be under-predicted using SimCYP. For instance, carbamazepine resulted in a potent clinical interaction (AUCR = 0.1) but the model predicted an AUCR of 0.54 (Table 5). Similarly, efavirenz, ritonavir and rifampin were clinical inducers (AUCR 0.44-0.78) but the model

predicted an AUCR = 0.79-0.94 (Table 6). The clinical non-inducers, cimetidine, nelfinavir, and teriflunomide were accurately characterized using the mechanistic dynamic modeling approach in SimCYP. There were no false positives observed. However, in one trial ritonavir resulted in a false positive (AUCR predicted = 0.79, observed = 0.98). In the case of the mechanistic dynamic model for efavirenz, there were no clinical trials where potent induction was observed and only 6 of 16 trials had moderate induction results (AUCR 0.2-0.8). Clinical non-inducers, ezetimibe, indinavir, and saquinavir were accurately characterized using the mechanistic dynamic modeling approach. The predicted AUCR for carbamazepine was slightly lower (0.48) than the observed AUCR of 0.64. Of note, there were 5 false negative predictions using this approach, four for rifampin, and one for nevirapine.

DISCUSSION

The U.S. FDA and EMA DDI guidance documents recommend a dedicated clinical CYP2B6 induction study if the NME is shown to be a CYP2B6 inducer *in vitro*, unless the induction potential can be ruled out using predictive mathematical models (EMA, 2012; FDA, 2012). These models range from basic static to physiologically-based dynamic approaches, with increasing complexity towards the latter. The ability of such models to predict the CYP3A4 induction potential of drugs was previously established (Fahmi et al., 2008a & 2008b; Fahmi and Ripp, 2010b; Einolf et al., 2014, Vieira et al., 2014).

In this current study, the ability of IVIVE models to predict CYP2B6 induction potential was evaluated. The data presented here suggest that CYP2B6 IVIVE is not possible for the probe substrate bupropion due to the overall significant under-prediction of the clinical data, regardless of the mathematical model used (Figures 1-4 and Table 5). A significant scatter and lack of correlation with bupropion using the RIS model, suggests a lack of sensitivity perhaps due to the

DMD Fast Forward. Published on July 15, 2016 as DOI: 10.1124/dmd.116.071076
This article has not been copyedited and formatted. The final version may differ from this version.

low f_m CYP2B6 for bupropion. When the static or dynamic models were applied, the predicted AUCRs were inconsistent with the observed clinical data, and an overall under-prediction was noticed when the observed AUCR values were less than 0.8.

In general, a relatively better IVIVE was achieved for efavirenz compared to bupropion, and there was less misclassification of the inducers according to the cutoff criteria (AUCR of 0.8). With the Net Effect model, however, a scaling factor (d=0.50) was applied to efavirenz data in order to achieve a reasonable correlation without any false negatives (GMFE 1.09). For efavirenz, PBPK modeling resulted in a reasonable performance in predicting CYP2B6 induction (GMFE 1.22) (Table 6). However misclassification leading to false negative predictions with nevirapine and rifampin was observed.

There are several factors that may explain the poor IVIVE for CYP2B6 in this study. One of the major challenges in predicting CYP2B6 induction was the lack of selective, sensitive and IVIVE validated clinical probe substrates of this enzyme. Although efavirenz and bupropion have been reported to be good probe substrates for CYP2B6 in the literature and in regulatory documents, (Walsky et al., 2006) limited data exists to support a high f_m (>0.8) for these two probes. Walsky et al. reported an estimated f_m of 0.9 for efavirenz based on a combination of clinical and *in vitro* data. However, based on literature information, (Faucette et al., 2000; Hesse et al., 2000; Ward et al., 2003; Walsky et al., 2006), the CYP2B6 inhibitor clopidogrel (with an *in vitro* CYP2B6 IC_{50} of 0.021 µM) was predicted to cause strong inhibition clinically (predicted AUCR 8.8) if f_m CYP2B6 was assumed to be 0.9. However, clopidogrel clinical DDI data with both bupropion and efavirenz showed minimal interaction (observed AUCR values of 1.36 and 1.26), respectively) (Turpeinen et al., 2005; Jiang et al., 2013), suggesting that efavirenz f_m may not be as high as originally estimated. Additionally, recent reports also suggest that bupropion and

DMD Fast Forward. Published on July 15, 2016 as DOI: 10.1124/dmd.116.071076
This article has not been copyedited and formatted. The final version may differ from this version.

efavirenz have lower f_m CYP2B6 values of $\leq$0.6 (Ke et al., 2016). This low f_m for CYP2B6 clinical probe substrates is also complicated by overlapping metabolism of competing pathways such as CYP3A4, CYP2C19, 11β–HSD and carbonyl reductase for bupropion (Hesse et al., 2006; Molnari et al., 2012; Sage et al., 2015) and CYP3A4, CYP2A6 and UGT2B7 for efavirenz (Ward et al., 2003; Kwara et al., 2011). It was also reported that efavirenz may serve as a better probe substrate for CYP2B6 clinical studies than bupropion when the ratio of 8,14-dihydroxyefavirenz to efavirenz was used as a phenotypic index for CYP2B6 activity *in vivo* (Jiang et al., 2013).

The auto-induction upon multiple dose administration of efavirenz, results in induction of CYP2B6 and CYP3A4-mediated metabolism. This auto-induction leads to an apparently lower magnitude of DDI when another inducer is co-administered, compared to when efavirenz is administered as a single dose following the perpetrator. For example, the magnitude of AUCR change was larger for efavirenz when administered as a single dose (Table 2) in the presence of rifampin (AUCR 0.44-0.61) compared to studies in which both were co-administered for multiple doses (AUCR 0.63-0.82). This is because comparing steady state exposures of efavirenz with and without rifampin takes into account auto-induction by efavirenz compared to day 1 when exposure is higher than steady state. As illustrated by the HepatoPac data (Table 4), the complexity of mimicking the steady state with non-selective marker substrates arises, due to co-induction of the CYP3A4 pathway and compensatory pathways that manifest when each pathway is inhibited. The fraction metabolized through each pathway is subject to these complex interactions. Therefore, selective marker substrates for CYP2B6 (f_m >0.9) are needed to better model steady state conditions.

DMD Fast Forward. Published on July 15, 2016 as DOI: 10.1124/dmd.116.071076
This article has not been copyedited and formatted. The final version may differ from this version.

Genetic polymorphisms also play a role in inter-individual variability of bupropion (Hesse et al., 2006) and efavirenz pharmacokinetics (Zanger et al., 2013), and their responses to inhibitors and inducers (Weerawat et al., 2013). It was also shown that the magnitude of reduction of efavirenz concentrations after multiple dosing was genotype dependent, where subjects with CYP2B6*1/*1 genotype (extensive metabolizer) had the largest decrease in their plasma concentrations relative to other CYP2B6 genotypes (Ngaimisi et al., 2010; Ngaimisi et al., 2011). This is similar to what have been observed previously with CYP2C9 polymorphisms (Lin et al., 2015).

The inducers used in clinical DDI trials (carbamazepine, efavirenz, nevirapine, rifampin and ritonavir) are not selective inducers for CYP2B6, but are known to induce both CYP2B6 and CYP3A4 *in vitro* and *in vivo* (Fahmi et al., 2010a; Fahmi and Ripp, 2010b). For example, *in vitro* data showed that the ratio of CYP3A4 to CYP2B6 maximum induction (E_{max}) was generally higher than unity for all clinical inducers (Table 3), suggesting that CYP3A4 induction may always predominate over CYP2B6. The induction potency of the inducers towards each enzyme as determined by the *in vitro* EC_{50} values was also overlapping between CYP2B6 and CYP3A4 and varied to the same extent across several inducers. For these precipitants, the *in vitro* observations are supported by the clinical DDI data where induction-mediated DDIs with probe substrates of both CYP2B6 and CYP3A4 (Einolf et al., 2013) have been reported to be significant (AUCR 0.65-0.10). To date, selective clinical CYP2B6 inducers have not been identified *in vitro* or *in vivo*. Since all of the tested compounds show co-induction of CYP2B6 and CYP3A4, it would be reasonable to question the value of generating CYP2B6 clinical DDI data, especially since confidence in predicting clinical CYP2B6 DDI is challenged by the lack of selective CYP2B6 inducers and substrates.

DMD Fast Forward. Published on July 15, 2016 as DOI: 10.1124/dmd.116.071076
This article has not been copyedited and formatted. The final version may differ from this version.

In addition, there is a systematic difference in the induction magnitude observed with bupropion vs efavirenz, when the same precipitants (rifampin and carbamazepine) were co-administered with each of these substrates. The clinically reported AUCR values (Table 2) were smaller for bupropion (AUCR range 0.10-0.52) relative to efavirenz (AUCR range 0.44-0.64), indicating a larger DDI with bupropion as a victim drug with these inducers. The stronger DDI with bupropion could be rationalized by the co-induction of CYP3A4 and CYP2B6 and a relatively larger contribution of CYP3A4 to its metabolism as compared with efavirenz.

There are relatively few pharmaceuticals where CYP2B6 is the major contributor to total clearance (Turpeinen et al., 2012). The clinical dataset used for this analysis contained multiple examples where competing inhibition could mask potential induction of CYP3A4 if used as a surrogate perpetrator for CYP2B6 induction (itraconazole, nelfinavir, ritonavir and saquinavir). .

Given the current limitations in establishing IVIVE for CYP2B6 induction, alternative strategies may be applied as follows. For NMEs that exhibit CYP2B6 and CYP3A4 induction *in vitro*, a clinical CYP3A4 DDI study could serve as a surrogate for identifying the potential risk for CYP2B6 induction in the clinic (unless confounded by TDI), since induction with sensitive CYP3A4 substrates with all known clinical CYP3A4 inducers (described in this paper) results in changes in AUC much greater than those for bupropion and efavirenz. Practically, after generating *in vitro* EC_{50} and E_{max} values for CYP2B6 and CYP3A4 utilizing hepatocytes from three donors, modeling of CYP3A4 *in vitro* data using established IVIVE methods would determine whether clinical induction assessment for CYP3A4 is necessary. If induction of CYP3A4 is predicted and clinical induction is observed with a sensitive clinical probe substrate

(i.e. midazolam), validation of the CYP3A4 IVIVE model can be performed and used to leverage the CYP2B6 *in vitro* induction data in order to perform a clinical risk assessment for CYP2B6 (i.e. calibration based on the *in vitro* E_{max} ratio [CYP3A4/CYP2B6] to estimate a scaling factor). If the CYP3A4 clinical induction study is negative or mild it can be concluded that the likely hood of CYP2B6 clinical induction is low and a clinical study for CYP2B6 may not be warranted. For an NME for which CYP3A4 inhibition (reversible or TDI) is observed *in vitro* along with induction, the potential for CYP2B6 induction may need an independent investigation.

The potential need for a clinical assessment of CYP2B6 induction may depend on other factors, such as the concomitant administration of CYP2B6 substrates in the targeted patient population or non-chronic treatment duration and regimens for the NME. If a more selective CYP2B6 clinical probe would be identified or if CYP2B6 *in vitro* induction is observed in the absence of CYP3A4 induction, an investigation of CYP2B6 induction clinically with a dedicated DDI study could prove useful using single dose efavirenz as a substrate.

Overall, this study highlights the challenges in using current IVIVE approaches for evaluating CYP2B6 induction potential of new molecular entities, and proposes alternatives strategies to assess the DDI risk on a case by case basis.

ACKNOWLEDGMENTS

The authors thank Georgy Hartman and Pramila Kumari (Merck Research Laboratories), Lai Wang, and Dung Yu Chun (Novartis), Philip Clark and Dung Nguyen (GlaxoSmithKline), Ming Zheng (BMS), Anitha Saravanakumar, Jian Lin, Kelly Nulick, Zhiwu Lin, Nat Johnson, Xin Yang, and Kimberly Lapham (Pfizer, Inc.), and Jun Sun (Abbvie Inc.) for generating *in vitro* data and/ or collating in vivo data and/or contribution in SimCYP analysis.

The authors also like to thank reviewers from IQ DMLG, and Lei Zhang, Ping Zhao and Shiew-Mei Huang (US Food and Drug Administration) for the valuable discussion.

The views expressed in this article are those of the authors and do not necessarily reflect official views of the EMA or the US Food and Drug Administration.

AUTHOR CONTRIBUTIONS

Participated in research design: Fahmi, Shebley, Palamanda, Sinz, Ramsden, Einolf, Chen, Wang.

Conducted experiments: Fahmi, Shebley, Palamanda, Sinz, Ramsden, Einolf, Chen, Wang.

Contributed new reagents or analytic tools: Fahmi, Shebley, Palamanda, Sinz, Ramsden, Einolf, Chen, Wang.

Performed data analysis: Fahmi, Shebley, Palamanda, Sinz, Ramsden, Einolf, Chen, Wang.

Wrote or contributed to the writing of the manuscript: Fahmi, Shebley, Palamanda, Sinz, Ramsden, Einolf, Chen, Wang.

References

Bjornsson TD, Callaghan JT, Einolf HJ, Fischer V, Gan L, Grimm S, Kao J, King SP, Miwa G, Ni L, Kumar G, McLeod J, Obach RS, Roberts S, Roe A, Shah A, Snikeris F (2003) The conduct of in vitro and in vivo drug-drug interaction studies: a Pharmaceutical Research and Manufacturers of America (PhRMA) perspective. *Drug Metab Dispos* **31:**815-832.

Cho DY, Ogburn ET, Jones D, and Desta Z (2011) Contribution of N-glucuronidation to efavirenz elimination in vivo in the basal and rifampin-induced metabolism of efavirenz. *Antimicrob Agents Chemother* **55:**1504-1509.

Chung JY, Cho JY, Lim HS, Kim JR, Yu KS, Lim KS, Shin SG, and Jang IJ (2011) Effects of pregnane X receptor (NR1I2) and CYP2B6 genetic polymorphisms on the induction of bupropion hydroxylation by rifampin. *Drug Metab Dispos* **39:**92-97.

Court MH, Almutairi FE, Greenblatt DJ, Hazarika S, Sheng H, Klein K, Zanger UM, Bourgea J, Patten CJ, and Kwara A (2014) Isoniazid mediates the CYP2B6*6 genotype-dependent interaction between efavirenz and antituberculosis drug therapy through mechanism-based inactivation of CYP2A6. *Antimicrobial agents and chemotherapy* **58:**4145-4152.

Court MH, Duan SX, Hesse LM, Venkatakrishnan K, and Greenblatt DJ (2001) Cytochrome P-450 2B6 is responsible for interindividual variability of propofol hydroxylation by human liver microsomes. *Anesthesiology* **94:**110-119.

di Iulio J, Fayet A, Arab-Alameddine M, Rotger M, Lubomirov R, Cavassini M, Furrer H, Gunthard HF, Colombo S, Csajka C, Eap CB, Decosterd LA, Telenti A (2009) In vivo analysis of efavirenz metabolism in individuals with impaired CYP2A6 function. *Pharmacogenetics and genomics* **19:**300-309.

Einolf HJ, Chen L, Fahmi OA, Gibson CR, Obach RS, Shebley M, Silva J, Sinz MW, Unadkat JD, Zhang L, and Zhao P (2014) Evaluation of Various Static and Dynamic Modeling Methods to Predict Clinical CYP3A Induction Using In Vitro CYP3A4 mRNA Induction Data. *Clin Pharmacol Ther* **95:**179-188.

Ekins S, Vandenbranden M, Ring BJ, Gillespie JS, Yang TJ, Gelboin HV, and Wrighton SA (1998) Further characterization of the expression in liver and catalytic activity of CYP2B6. *J Pharmacol Exp Ther* **286:**1253-1259.

European Medicines Agency (EMA, 2012). Guideline on the investigation of drug interactions. http://www.ema.europa.eu/docs/en_GB/document_library/Scientific_guideline/2012/07/WC500129606.

Fahmi OA, Boldt S, Kish M, Obach RS, and Tremaine LM (2008a) Prediction of drug-drug interactions from in vitro induction data: application of the relative induction score approach using cryopreserved human hepatocytes. *Drug Metab Dispos* **36:**1971-1974.

Fahmi OA, Maurer TS, Kish M, Cardenas E, Boldt S, and Nettleton D (2008b) A combined model for predicting CYP3A4 clinical net drug-drug interaction based on CYP3A4 inhibition, inactivation, and induction determined in vitro. *Drug Metab Dispos* **36:**1698-1708.

Fahmi OA, Hurst S, Plowchalk D, Cook J, Guo F, Youdim K, Dickins M, Phipps A, Darekar A, Hyland R, and Obach RS (2009) Comparison of different algorithms for predicting clinical drug-drug interactions, based on the use of CYP3A4 in vitro data: predictions of compounds as precipitants of interaction. *Drug Metab Dispos* **37:**1658-1666.

Fahmi OA, Kish M, Boldt S, and Obach RS (2010a) Cytochrome P450 3A4 mRNA is a more reliable marker than CYP3A4 activity for detecting pregnane X receptor-activated induction of drug-metabolizing enzymes. *Drug Metab Dispos* **38:**1605-1611.

Fahmi OA and Ripp SL (2010b) Evaluation of models for predicting drug-drug interactions due to induction. *Expert Opin Drug Metab Toxicol* **6:**1399-1416.

Faucette SR, Hawke RL, Lecluyse EL, Shord SS, Yan B, Laethem RM, and Lindley CM (2000) Validation of bupropion hydroxylation as a selective marker of human cytochrome P450 2B6 catalytic activity. *Drug Metab Dispos* **28:**1222-1230.

Faucette SR, Zhang TC, Moore R, Sueyoshi T, Omiecinski CJ, LeCluyse EL, Negishi M, and Wang H (2007) Relative activation of human pregnane X receptor versus constitutive androstane receptor defines distinct classes of CYP2B6 and CYP3A4 inducers. *J Pharmacol Exp Ther* **320:**72-80.

FDA US (2012). Guidance for Industry Drug Interaction Studies http://www.fda.gov/downloads/drugs/guidancecomplianceregulatoryinformation/guidances/ucm292362.

Hesse LM, Greenblatt DJ, von Moltke LL, and Court MH (2006) Ritonavir has minimal impact on the pharmacokinetic disposition of a single dose of bupropion administered to human volunteers. *J Clin Pharmacol* **46:**567-576.

Hesse LM, Venkatakrishnan K, Court MH, von Moltke LL, Duan SX, Shader RI, and Greenblatt DJ (2000) CYP2B6 mediates the in vitro hydroxylation of bupropion: potential drug interactions with other antidepressants. *Drug Metab Dispos* **28:**1176-1183.

Hidestrand M, Oscarson M, Salonen JS, Nyman L, Pelkonen O, Turpeinen M, and Ingelman-Sundberg M (2001) CYP2B6 and CYP2C19 as the major enzymes responsible for the metabolism of selegiline, a drug used in the treatment of Parkinson's disease, as revealed from experiments with recombinant enzymes. *Drug Metab Dispos* **29:**1480-1484.

Ji P, Damle B, Xie J, Unger SE, Grasela DM, and Kaul S (2008) Pharmacokinetic interaction between efavirenz and carbamazepine after multiple-dose administration in healthy subjects. *J Clin Pharmacol* **48:**948-956.

Jiang F, Desta Z, Shon JH, Yeo CW, Kim HS, Liu KH, Bae SK, Lee SS, Flockhart DA, and Shin JG (2013) Effects of clopidogrel and itraconazole on the disposition of efavirenz and its hydroxyl

metabolites: exploration of a novel CYP2B6 phenotyping index. *Br J Clin Pharmacol* **75:**244-253.

Ke A, Barter Z,Yeo K, Almond L. (2016) Toward a Best Practice Approach in PBPK Modeling: Case Example of Developing a Unified Efavirenz Model Accounting for Induction of CYPs 3A4 and 2B6. *CPT: Pharmacometrics & Systems Pharmacology In Press doi:101002/psp412088.*

Ketter TA, Jenkins JB, Schroeder DH, Pazzaglia PJ, Marangell LB, George MS, Callahan AM, Hinton ML, Chao J, and Post RM (1995) Carbamazepine but not valproate induces bupropion metabolism. *J Clin Psychopharmacol* **15:**327-333.

Kharasch ED, Mitchell D, and Coles R (2008a) Stereoselective bupropion hydroxylation as an in vivo phenotypic probe for cytochrome P4502B6 (CYP2B6) activity. *J Clin Pharmacol* **48:**464-474.

Kharasch ED, Mitchell D, Coles R, and Blanco R (2008b) Rapid clinical induction of hepatic cytochrome P4502B6 activity by ritonavir. *Antimicrob Agents Chemother* **52:**1663-1669.

Kirby BJ, Collier AC, Kharasch ED, Dixit V, Desai P, Whittington D, Thummel KE, and Unadkat JD (2011) Complex drug interactions of HIV protease inhibitors: in vivo induction and in vitro to in vivo correlation of induction of cytochrome P450 1A2, 2B6, and 2C9 by ritonavir or nelfinavir. *Drug Metab Dispos* **39:**2329-2337.

Kustra R, Corrigan B, Dunn J, Duncan B, and Hsyu PH (1999) Lack of effect of cimetidine on the pharmacokinetics of sustained-release bupropion. *J Clin Pharmacol* **39:**1184-1188.

Kwara A, Cao L, Yang H, Poethke P, Kurpewski J, Tashima KT, Mahjoub BD, Court MH, and Peloquin CA (2014) Factors associated with variability in rifampin plasma pharmacokinetics and the relationship between rifampin concentrations and induction of efavirenz clearance. *Pharmacotherapy* **34:**265-271.

Kwara A, Lartey M, Sagoe KW, Kenu E, and Court MH (2009) CYP2B6, CYP2A6 and UGT2B7 genetic polymorphisms are predictors of efavirenz mid-dose concentration in HIV-infected patients. *Aids* **23:**2101-2106.

Kwara A, Tashima KT, Dumond JB, Poethke P, Kurpewski J, Kashuba AD, Court MH, and Greenblatt DJ (2011) Modest but variable effect of rifampin on steady-state plasma pharmacokinetics of efavirenz in healthy African-American and Caucasian volunteers. *Antimicrob Agents Chemother* **55:**3527-3533.

Lehmann JM, McKee DD, Watson MA, Willson TM, Moore JT, and Kliewer SA (1998) The human orphan nuclear receptor PXR is activated by compounds that regulate CYP3A4 gene expression and cause drug interactions. *J Clin Invest* **102:**1016-1023.

Lin J, Zhang Y, Zhou H, Wang X, and Wang W (2015) CYP2C9 Genetic Polymorphism is a Potential Predictive Marker for the Efficacy of Rosuvastatin Therapy. *Clin Lab* **61:**1317-1324.

Loboz KK, Gross AS, Williams KM, Liauw WS, Day RO, Blievernicht JK, Zanger UM, and McLachlan AJ (2006) Cytochrome P450 2B6 activity as measured by bupropion hydroxylation: effect of induction by rifampin and ethnicity. *Clin Pharmacol Ther* **80:**75-84.

Lopez-Cortes LF, Ruiz-Valderas R, Viciana P, Alarcon-Gonzalez A, Gomez-Mateos J, Leon-Jimenez E, Sarasanacenta M, Lopez-Pua Y, and Pachon J (2002) Pharmacokinetic interactions between efavirenz and rifampicin in HIV-infected patients with tuberculosis. *Clin Pharmacokinet* **41:**681-690.

Ma Q, Forrest A, Rosenkranz SL, Para MF, Yarasheski KE, Reichman RC, Morse GD, and Actg A Protocol Team DN (2008) Pharmacokinetic interaction between efavirenz and dual protease inhibitors in healthy volunteers. *Biopharm Drug Dispos* **29:**91-101.

Matteelli A, Regazzi M, Villani P, De Iaco G, Cusato M, Carvalho AC, Caligaris S, Tomasoni L, Manfrin M, Capone S, and Carosi G (2007) Multiple-dose pharmacokinetics of efavirenz with and without the use of rifampicin in HIV-positive patients. *Curr HIV Res* **5:**349-353.

Meyer HE, Oswald S, Bresser C, Nassif A, Modess C, Desta Z, Ogburn ET, Marinova M, Lutjohann D, Spielhagen C, Nauck M, Kroemer HK, and Siegmund W (2012) Compartment-specific gene regulation of the CAR inducer efavirenz in vivo. *Clin Pharmacol Ther* **92:**103-111.

Molnari JC and Myers AL (2012) Carbonyl reduction of bupropion in human liver. *Xenobiotica* **42:**550-561.

Ngaimisi E, Mugusi S, Minzi O, Sasi P, Riedel KD, Suda A, Ueda N, Janabi M, Mugusi F, Haefeli WE, Bertilsson L, Burhenne J, and Aklillu E (2011) Effect of rifampicin and CYP2B6 genotype on long-term efavirenz autoinduction and plasma exposure in HIV patients with or without tuberculosis. *Clin Pharmacol Ther* **90:**406-413.

Ngaimisi E, Mugusi S, Minzi OM, Sasi P, Riedel KD, Suda A, Ueda N, Janabi M, Mugusi F, Haefeli WE, Burhenne J, and Aklillu E (2010) Long-term efavirenz autoinduction and its effect on plasma exposure in HIV patients. *Clin Pharmacol Ther* **88:**676-684.

Ogburn ET, Jones DR, Masters AR, Xu C, Guo Y, and Desta Z (2010) Efavirenz primary and secondary metabolism in vitro and in vivo: identification of novel metabolic pathways and cytochrome P450 2A6 as the principal catalyst of efavirenz 7-hydroxylation. *Drug Metab Dispos* **38:**1218-1229.

Oswald S, Meyer zu Schwabedissen HE, Nassif A, Modess C, Desta Z, Ogburn ET, Mostertz J, Keiser M, Jia J, Hubeny A, Ulrich A, Runge D, Marinova M, Lutjohann D, Kroemer HK, and Siegmund W (2012) Impact of efavirenz on intestinal metabolism and transport: insights from an interaction study with ezetimibe in healthy volunteers. *Clin Pharmacol Ther* **91:**506-513.

Park J, Vousden M, Brittain C, McConn DJ, Iavarone L, Ascher J, Sutherland SM, and Muir KT (2010) Dose-related reduction in bupropion plasma concentrations by ritonavir. *J Clin Pharmacol* **50:**1180-1187.

Ramsden D, Zhou J, and Tweedie DJ (2015) Determination of a Degradation Constant for CYP3A4 by Direct Suppression of mRNA in a Novel Human Hepatocyte Model, HepatoPac. *Drug Metab Dispos* **43:**1307-1315.

Robertson SM, Maldarelli F, Natarajan V, Formentini E, Alfaro RM, and Penzak SR (2008) Efavirenz induces CYP2B6-mediated hydroxylation of bupropion in healthy subjects. *J Acquir Immune Defic Syndr* **49:**513-519.

Roy P, Yu LJ, Crespi CL, and Waxman DJ (1999) Development of a substrate-activity based approach to identify the major human liver P-450 catalysts of cyclophosphamide and ifosfamide activation based on cDNA-expressed activities and liver microsomal P-450 profiles. *Drug Metab Dispos* **27:**655-666.

Sage JS, Le H, Chang J, Isoherrane N (2015) New Metabolic Pathways of Bupropion in vivo Reveal an Important Role of CYP2C19 and 11B-HSD in Bupropion Clearance; CYP2B6 Contribution to Bupropion Clearance is Minor. *ACS Med Chem Letters, e Pub June 17, 2016 DOI: 10.1021/acsmedchemlett.6b00189.*

Sheedy PF, 2nd, Stephens DH, Hattery RR, MacCarty RL, and Williamson B, Jr. (1977) Computed tomography of the pancreas. *Radiol Clin North Am* **15:**349-366.

Smith PF, Robbins GK, Shafer RW, Wu H, Yu S, Hirsch MS, Merigan TC, Park JG, Forrest A, Fischl MA, Morse GD, and Team A (2005) Pharmacokinetics of nelfinavir and efavirenz in antiretroviral-naive, human immunodeficiency virus-infected subjects when administered alone or in combination with nucleoside analog reverse transcriptase inhibitors. *Antimicrob Agents Chemother* **49:**3558-3561.

Sueyoshi T, Kawamoto T, Zelko I, Honkakoski P, and Negishi M (1999) The repressed nuclear receptor CAR responds to phenobarbital in activating the human CYP2B6 gene. *J Biol Chem* **274:**6043-6046.

Tolson AH and Wang H (2010) Regulation of drug-metabolizing enzymes by xenobiotic receptors: PXR and CAR. *Adv Drug Deliv Rev* **62:**1238-1249.

Turpeinen M, Tolonen A, Uusitalo J, Jalonen J, Pelkonen O, and Laine K (2005) Effect of clopidogrel and ticlopidine on cytochrome P450 2B6 activity as measured by bupropion hydroxylation. *Clin Pharmacol Ther* **77:**553-559.

Turpeinen M and Zanger UM (2012) Cytochrome P450 2B6: function, genetics, and clinical relevance. *Drug Metabol Drug Interact* **27:**185-197.

Veldkamp AI, Harris M, Montaner JS, Moyle G, Gazzard B, Youle M, Johnson M, Kwakkelstein MO, Carlier H, van Leeuwen R, Beijnen JH, Lange JM, Reiss P, and Hoetelmans RM (2001) The steady-state pharmacokinetics of efavirenz and nevirapine when used in combination in human immunodeficiency virus type 1-infected persons. *J Infect Dis* **184:**37-42.

Vieira ML, Kirby B, Ragueneau-Majlessi I, Galetin A, Chien JY, Einolf HJ, Fahmi OA, Fischer V, Fretland A, Grime K, Hall SD, Higgs R, Plowchalk D, Riley R, Seibert E, Skordos K, Snoeys J, Venkatakrishnan K, Waterhouse T, Obach RS, Berglund EG, Zhang L, Zhao P, Reynolds KS, and Huang SM (2014) Evaluation of various static in vitro-in vivo extrapolation models for risk assessment of the CYP3A inhibition potential of an investigational drug. *Clin Pharmacol Ther* **95:**189-198.

Villani P, Regazzi MB, Castelli F, Viale P, Torti C, Seminari E, and Maserati R (1999) Pharmacokinetics of efavirenz (EFV) alone and in combination therapy with nelfinavir (NFV) in HIV-1 infected patients. *Br J Clin Pharmacol* **48:**712-715.

Walsky RL, Astuccio AV, and Obach RS (2006) Evaluation of 227 drugs for in vitro inhibition of cytochrome P450 2B6. *J Clin Pharmacol* **46:**1426-1438.

Wang H and Tompkins LM (2008) CYP2B6: new insights into a historically overlooked cytochrome P450 isozyme. *Curr Drug Metab* **9:**598-610.

Ward BA, Gorski JC, Jones DR, Hall SD, Flockhart DA, and Desta Z (2003) The cytochrome P450 2B6 (CYP2B6) is the main catalyst of efavirenz primary and secondary metabolism: implication for HIV/AIDS therapy and utility of efavirenz as a substrate marker of CYP2B6 catalytic activity. *J Pharmacol Exp Ther* **306:**287-300.

Weerawat W, Pichitlamken J, and Subsombat P (2013) A generic discrete-event simulation model for outpatient clinics in a large public hospital. *J Healthc Eng* **4:**285-305.

Xie W, Barwick JL, Simon CM, Pierce AM, Safe S, Blumberg B, Guzelian PS, and Evans RM (2000) Reciprocal activation of xenobiotic response genes by nuclear receptors SXR/PXR and CAR. *Genes Dev* **14:**3014-3023.

Yenny, Nafrialdi, Djoerban Z, and Setiabudy R (2011) Pharmacokinetic interaction between efavirenz and rifampicin in healthy volunteers. *Int J Clin Pharmacol Ther* **49:**162-168.

Zanger UM and Klein K (2013) Pharmacogenetics of cytochrome P450 2B6 (CYP2B6): advances on polymorphisms, mechanisms, and clinical relevance. *Front Genet* **4:**24.

Zanger UM, Klein K, Saussele T, Blievernicht J, Hofmann MH, and Schwab M (2007) Polymorphic CYP2B6: molecular mechanisms and emerging clinical significance. *Pharmacogenomics* **8:**743-759.

DMD Fast Forward. Published on July 15, 2016 as DOI: 10.1124/dmd.116.071076
This article has not been copyedited and formatted. The final version may differ from this version.

Legends for Figures

Figure 1: Prediction of drug–drug interactions (DDI), using the basic R3 model where *C*max equal to total *C*max, with efavirenz (circles), and bupropion (Squares) as the victim drugs.

Figure 2: Prediction of drug–drug interactions (DDI) using the relative induction score (RIS) model. Panel A with efavirenz and Panel B with bupropion, as the victim drugs.

Figure 3: Net effect model predicted DDI (AUCR) compared with Observed DDI (AUCR), Panel A with efavirenz and Panel B with bupropion, as the victim drugs.

Figure 4: SimCYP model predicted DDI (AUCR) compared with Observed DDI (AUCR), Panel A with efavirenz and Panel B with bupropion, as the victim drugs.

Table 1: Summary of the *in vivo* bupropion DDI clinical studies used for predictions

Precipitant	Precipitant Dose (duration)	Precipitant Dose interval	Bupropion Victim Drug Dose	Bupropion Dose interval	Observed DDI (AUCR)	References
Carbamazepine	942 mg (W)	QD	150 mg	SD	0.10	(Ketter et al., 1995)
Cimetidine	800 mg (1d)	QD	300 mg	SD	1.05	(Kustra et al., 1999)
Efavirenz	600 mg (15d)	QD	150 mg	SD	0.45	(Robertson et al., 2008)
Nelfinavir	1250 mg(14d)	BID	150 mg	SD	0.92	(Kirby et al., 2011)
Rifampin	600 mg (7d)	QD	150 mg	SD	0.33	(Chung et al., 2011)
Rifampin	600 mg (10d)	QD	150 mg	SD	0.33	(Loboz et al., 2006)
Rifampin	600 mg(10d)	QD	150 mg	SD	0.52	(Kharasch et al., 2008a)
Ritonavir	100 mg(23d)	BID	150 mg	SD	0.78	(Park et al., 2010)
Ritonavir	200-400 mg (14d)	TID	150 mg	SD	0.67	(Kirby et al., 2011)
Ritonavir	600 mg (23d)	BID	150 mg	SD	0.34	(Park et al., 2010)
Ritonavir	200-300 mg (18d)	BID	150 mg	SD	0.98	(Kharasch et al., 2008b)
Ritonavir	200-300 mg (3d)	BID	150 mg	SD	0.84	(Kharasch et al., 2008b)
Ritonavir	200 mg (2d)	BID	75 mg	SD	1.2	(Hesse et al., 2006)
Teriflunomide	14-70 mg (14d)	QD	150 mg	SD	0.91	(Sheedy et al., 1977)

Three times a day dose (TID), twice a day dose (BID), once a day dose (QD), day (d) and week (W)

Table 2: Summary of the *in vivo* efavirenz DDI clinical studies used for predictions

Precipitant	Precipitant Dose (duration)	Dose interval	Efavirenz Victim Drug Dose (duration)	Efavirenz Dose interval	Observed DDI (AUCR)	References
Carbamazepine	200-400 mg (21d)	QD	600 mg (35d)	QD	0.64	(Ji et al., 2008)
Ezetimibe	10 mg (11d)	QD	400 mg	SD	0.91	(Meyer et al., 2012)
Ezetimibe	10 mg (24d)	QD	400 mg	SD	1.1	(Oswald et al., 2012)
Indinavir	1200 mg (7d)	BID	600 mg	SD	0.81	(Ma et al., 2008)
Itraconazole	200 mg (6d)	QD	200 mg	SD	1.0	(Jiang et al., 2013)
Nelfinavir	1250 mg (32w)	BID	600 mg (32w)	QD	0.83	(Smith et al., 2005)
Nelfinavir	1250 mg (7d)	BID	600 mg	SD	0.99	(Ma et al., 2008)
Nelfinavir	750 mg (>4w)	TID	600 mg (>4w)	QD	1.1	(Villani et al., 1999)
Nevirapine	400 mg (4w)	QD	600 mg(6w)	QD	0.71	(Veldkamp et al., 2001)
Rifampin	450 mg (7d)	QD	600 mg	SD	0.61	(Yenny et al., 2011)
Rifampin	600 mg (10d)	QD	600 mg	SD	0.44	(Cho et al., 2011)
Rifampin	600 mg (w)	QD	600-800 mg (w)	QD	0.63*	(Matteelli et al., 2007)
Rifampin	10.5 mg/kg (7d)	QD	600 mg (14d)	QD	0.78	(Lopez-Cortes et al., 2002)
Rifampin	600 mg (8d)	QD	600 mg (8d)	QD	0.82	(Kwara et al., 2011)
Ritonavir	100 mg (7d)	BID	600 mg	SD	1.0	(Ma et al., 2008)
Saquinavir	1600 mg (7d)	BID	600 mg	SD	0.89	(Ma et al., 2008)

Three times a day dose (TID), twice a day dose (BID), once a day dose (QD), day (d) and week (W)

*observed fold-change in CL ($CL_{control}/CL_{induced}$)

Table 3: *In vitro* determined CYP3A4 and CYP2B6 DDI kinetic parameters

Precipitant	CYP3A4					CYP2B6			Ratio E_{max} CYP3A4/ CYP2B6	Ratio EC_{50} CYP3A4/ CYP2B6	Ratio E_{max}/EC_{50} CYP3A4/ CYP2B6
	K_i (µM)	K_I (µM)	k_{inact} (min^{-1})	E_{max}	EC_{50} (uM)	K_i (µM)	E_{max}	EC_{50} (µM)			
Carbamazepine	100	NA	NA	24.7	43.3	100	14.8	35.4	1.7	1.2	1.4
Cimetidine	100	NA	NA	NA	NA	100	NA	NA	NA	NA	NA
Efavirenz	20.6	NA	NA	19.6	4.59	2.7	10.8	1.62	1.8	2.8	0.64
Ezetimibe	3.3	1.1	0.06	4.90	10.2	5.5	3.48	6.68	1.4	1.5	0.92
Indinavir	0.4	NA	NA	8.30	16.5	40.0	2.29	15.2	3.6	1.1	3.3
Itraconazole	0.10	NA	NA	NA	NA	2.00	NA	NA	NA	NA	NA
Nelfinavir	0.9	2.3	0.10	15	1.51	6.5	4.14	1.43	3.7	1.1	3.4
Nevirapine	100	NA	NA	27	86.3	100	12.2	35.9	2.2	2.4	0.92
Rifampin	100	NA	NA	38	0.66	100	8.26	1.26	4.5	0.5	8.8
Ritonavir	0.004	0.07	0.21	20	1.40	2.3	5.73	0.87	3.5	1.6	2.2
Saquinavir	1.3	7.7	0.09	12	2.82	40.0	3.04	0.63	3.9	4.5	0.88
Teriflunomide	100	NA	NA	4.13	10.3	100	3.03	4.97	1.4	2.1	0.66
Phenobarbital	NA	NA	NA	21.1	347	NA	13.9	347	1.5	1.0	1.5
Phenytoin	NA	NA	NA	25.1	36	NA	14.9	14.3	1.7	2.5	0.67

Maximum fold increase (E_{max}), *In vitro* concentration of inducer that produced half the maximum induction (EC_{50}), Enzyme Inhibition Constant (K_i)- Inhibitor Concentration at 50% of kinact (K_I), Maximal Inactivation Rate (k_{inact}), Ratios of CYP3A4/CYP2B6 are based on the mean values of data generated from various lots, Not applicable (NA)

Table 4: Efavirenz metabolism using pre-induced HepatoPac with ^{14}C-efavirenz

	^{14}C-efavirenz % change relative to SC						
	CBZ	EFV	RIF	TIC	ERY	PCPAH	TEL
	CYP3A4/CYP2B6 Inducers			CYP2B6 Inhibitor	CYP3A4 Inhibitor	CYP2A6 Inhibitor	Pan-UGT Inhibitor
8-OH & its glucuronide conjugate	+60%	-17%	-22%	-76%	-54%	+16%	-16%
7-OH & its glucuronide conjugate	-26%	-33%	-37%	+88%	-22%	-94%	+48%
N-glucuronide	-60%	-37%	-60%	-59%	-54%	-79%	-98%
EFV	-52%	+17%	+19%	+40%	+47%	+13%	+7%

Human hepatocytes using HepatoPac Cells were initially induced with 10 µM **[**^{14}C]-efavirenz for 96-120 hrs (total radioactivity recovered ranged between 9.7-10.4 µM). Induced human HepatoPac plates were then incubated with and without inducers for additional 72 hr (10 µM RIF, 10 µM EFV and 100 µM CBZ) or co-incubated with inhibitors (50 µM ERY, 10 µM TIC, 10 µM TEL and 10 µM PCPAH). Solvent control (SC), CYP3A4/CYP2B6 Inducers; Carbamazepine (CBZ), efavirenz (EFV), rifampin (RIF). CYP2B6 Inhibitor; ticlopidine (TIC), CYP3A4 inhibitor; erythromycin (ERY), CYP2A6 inhibitor; trans-2-phenylcyclopropylamine hydrochloride (PCPAH) and *Pan*- UGT Inhibitor; telmisartan (TEL). % change relative to SC is calculated as =100-(Conc in presence of inhibitor or inducer/Conc in SC*100), (+) indicates increase in concentration relative to SC and (-) indicates decrease in concentration relative to SC.

DMD Fast Forward. Published on July 15, 2016 as DOI: 10.1124/dmd.116.071076
This article has not been copyedited and formatted. The final version may differ from this version.

Table 5: Summary of bupropion DDI predictions

	Predicted DDI (AUCR)			Observed DDI (AUCR)
Precipitant	**R3**	**Net effect**	**SimCYP**	**AUCR Change**
Carbamazepine	0.15	0.52	0.54	0.10
Cimetidine	0.99	1.0	1.07	1.05
Efavirenz	0.09	0.87	0.70	0.45
Nelfinavir	0.21	0.80	0.90	0.92
Rifampin (600 mg)	0.12	0.34	0.76	0.33
Rifampin (600 mg)	0.12	0.34	0.68	0.33
Rifampin (600 mg)	0.12	0.34	0.67	0.52
Ritonavir (100 mg)	0.20	0.95	0.90	0.78
Ritonavir (400 mg)	0.15	0.67	0.79	0.98
Ritonavir (600 mg)	0.16	0.75	0.74	0.34
Ritonavir (300 mg)	0.16	0.79	0.78	0.67
Ritonavir (300 mg-3d)	0.16	0.79	0.89	0.84
Ritonavir (200 mg-2d)	0.18	0.90	0.95	1.20
Teriflunomide	0.94	1.0	0.83	0.91
Prediction Error (GMFE)	3.45	1.39	1.50	
*% of True Positive	100%	75%	88%	
*% of True Negative	33%	67%	83%	
*% of False Positive	67%	33%	17%	
*% of False Negative	0%	25%	13%	

**Percent* of clinical trials that were predicted as false negative, false positive, true negative, or true positive with respect to induction based on the 0.8 fold cutoff criterion.

DMD Fast Forward. Published on July 15, 2016 as DOI: 10.1124/dmd.116.071076
This article has not been copyedited and formatted. The final version may differ from this version.

Table 6: Summary of efavirenz DDI predictions

	Predicted DDI (AUCR)				Observed DDI (AUCR)
Compound	**R3**	**RIS**	**Net Effect**	**SimCYP**	**AUCR Change**
Carbamazepine	0.15	0.69	0.64	0.48	0.64
Ezetimibe	0.87	0.99	1.00	1.00	0.91
Ezetimibe	0.87	0.99	1.00	1.00	1.1
Indinavir	0.53	0.82	0.93	1.12	0.81
Itraconazole	1.00	1.00	1.00	1.04	1.0
Nelfinavir	0.21	0.80	0.87	1.02	0.83
Nelfinavir	0.21	0.80	0.92	1.02	1.0
Nelfinavir	0.21	0.80	0.92	1.01	1.1
Nevirapine	0.20	0.69	0.65	0.86	0.71
Rifampin (450 mg)	0.13	0.66	0.48	0.81	0.61
Rifampin (600 mg)	0.12	0.65	0.44	0.79	0.44
Rifampin (600 mg)	0.12	NA	NA	0.87	0.63
Rifampin (10.5 mg/kg)	0.12	NA	NA	0.94	0.78
Rifampin (600 mg)	0.12	NA	NA	0.92	0.82
Ritonavir (100 mg)	0.20	0.94	0.97	0.85	1.0
Saquinavir	0.32	0.93	0.96	1.0	0.89
Prediction Error (GMFE)	3.25	1.12	1.09	1.22	
% of True Positive	100%	100%	100%	33%	
% of True Negative	19%	100%	100%	63%	
% of False Positive	70%	0%	0%	0%	
% of False Negative	0%	0%	0%	67%	

* NA: data were not included in the prediction since Efavirenz was administered as multiple doses prior to dosing with precipitant drugs. **Percent* of clinical trials that were predicted as false negative, false positive, true negative, or true positive with respect to induction based on the 0.8 fold cutoff criterion.

Figure 4

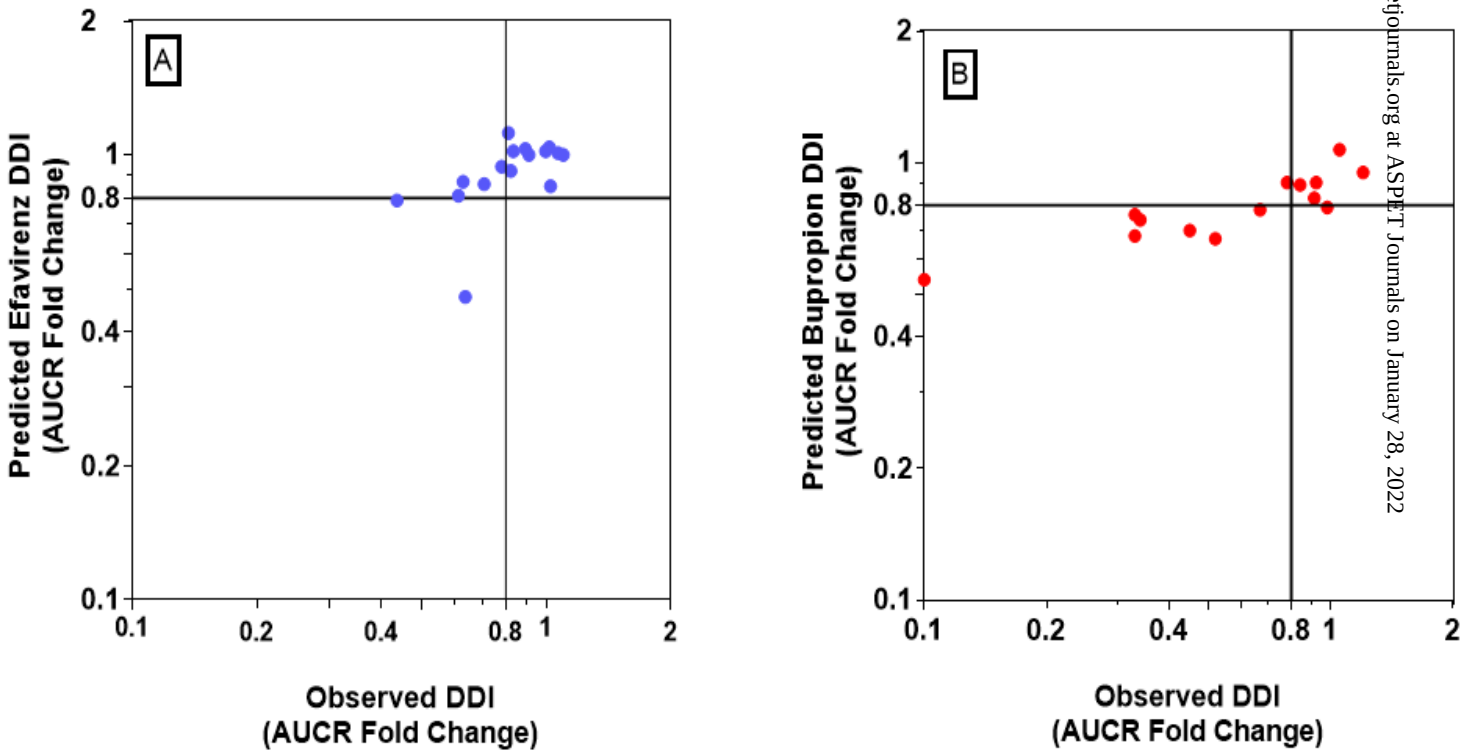

Figure 3

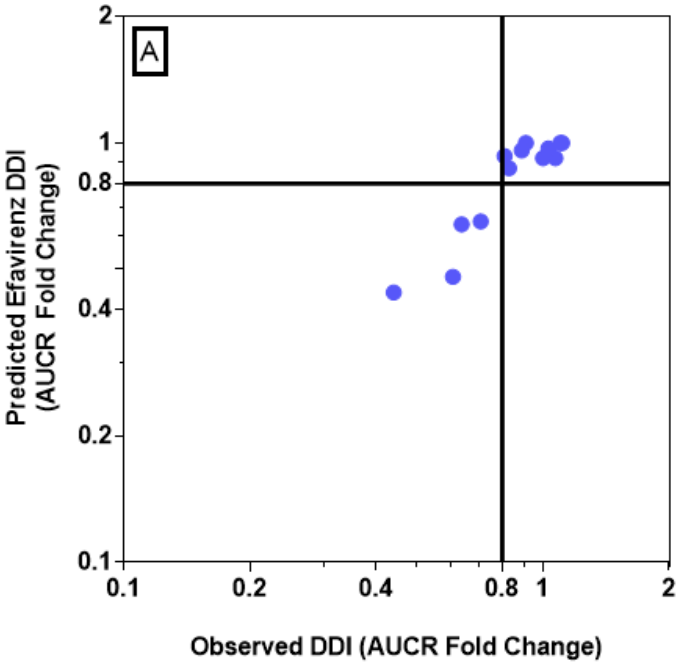

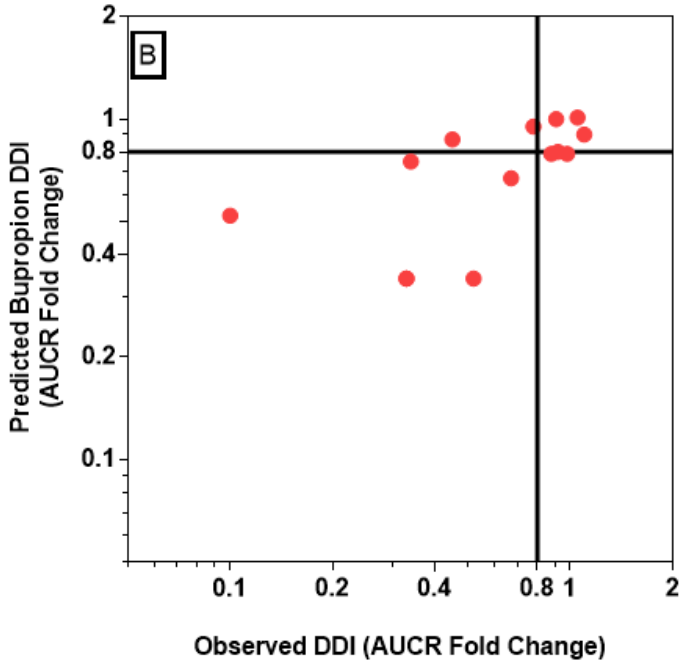

Figure 2

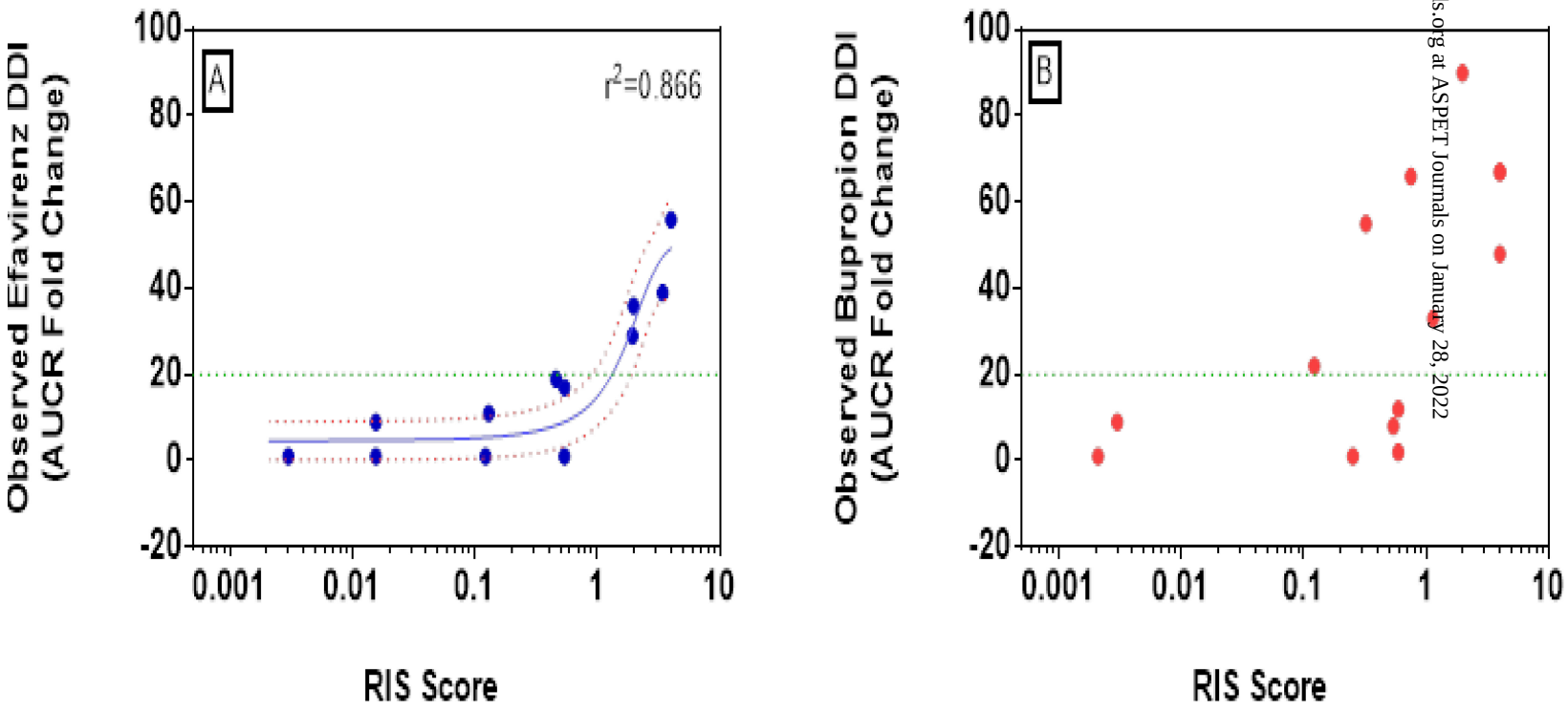

Figure 1